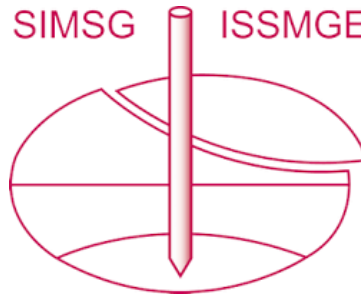


# INTERNATIONAL SOCIETY FOR SOIL MECHANICS AND GEOTECHNICAL ENGINEERING



*This paper was downloaded from the Online Library of the International Society for Soil Mechanics and Geotechnical Engineering (ISSMGE). The library is available here:*

<https://www.issmge.org/publications/online-library>

*This is an open-access database that archives thousands of papers published under the Auspices of the ISSMGE and maintained by the Innovation and Development Committee of ISSMGE.*

*The paper was published in the proceedings of the 7<sup>th</sup> International Conference on Earthquake Geotechnical Engineering and was edited by Francesco Silvestri, Nicola Moraci and Susanna Antonielli. The conference was held in Rome, Italy, 17 - 20 June 2019.*

## Experimental assessment of stiffness and damping in rubber-sand mixtures at various strain levels

J. Bernal-Sanchez, J. McDougall, D. Barreto, A. Marinelli & V. Dimitriadi  
*Edinburgh Napier University, Edinburgh, UK*

P. Anbazhagan  
*Indian Institute of Science, Bangalore, India*

M. Miranda  
*Universidad de Cantabria, Santander, Spain*

**ABSTRACT:** The dynamic properties of shredded rubber-soil mixtures (ShRm), comprising a sub-rounded quartz sand combined with small rubber shreds at 0, 10, 20, 30% by mass, were investigated. Testing ranged from small strain, in resonant column apparatus, to large strain, in cyclic triaxial, all at a frequency of 1 Hz with mean stress equal to 100 kPa. As observed by other workers, the shear stiffness of rubber soil mixtures decreases both (i) with rubber content and (ii) with shear strain. In contrast, increases in damping ratio are smallest at higher rubber contents. Shear modulus reduction behaviour for ShRm are shown to fit well for all percentage rubber contents, the functional form put forward by Darendeli (2001). Damping ratio was well-fitted by Darendeli up to a shear strain of about 0.2%, after which the variable trend shown by ShRm has been adjusted using the expression proposed by Phillips & Hashash (2009).

### 1 INTRODUCTION

The disposal of scrap tyres has become a major problem in many countries around the world with attendant environmental issues and health hazards. The high durability in addition to the strength of the vulcanised rubber has made the recovery of the material difficult, reasons explaining why the destination of used tyres has been typically landfills or stockpiles (ETRMA, 2015). Hence, a new landfill directive was approved in Europe banning both whole and shredded tyres from disposal in landfills (European Union, 2006).

Although end of life tyres (ELT) have been widely utilised as incinerator fuel, since the early 1990's, there has been a growing interest in recycling ELT in civil engineering applications. By combining a proportion of rubber particles with a mineral, typically sandy soil, to produce a new geomaterial, commonly known as a rubber-soil mixture (RSm) (Ghazavi, 2004, Sheikh et al., 2012, Anbazhagan et al., 2017). Because of its low unit weight, potential high shear strength, hydraulic conductivity and very high resilience, RSm have been employed as a lightweight backfill in retaining walls, soil reinforcement, or road embankments (Youwai & Bergado, 2003).

Soil foundations comprising of RSm have also been proposed to mitigate the action of seismic events (Tsang, 2008). This is based on the fact that adding particulate rubber to sand increases the damping ratio (Anastasiadis et al., 2012), attenuates horizontal accelerations (Kaneko et al., 2013) and improves the liquefaction resistance (Hazarika et al., 2008) revealing the good seismic performance of this material. As an average, 17 major earthquakes ( $M > 7.0$ ) occur and some 27,000 people die in seismic events annually (Spence et al., 2011). The majority of these casualties occur in high population density urban areas in the developing world mainly due to collapse of residential buildings which are seismically vulnerable, unable to afford the high cost of advanced structural isolation systems such as rubber bearings (Tsang,

2008). Hence, geotechnical seismic isolation systems were proposed as a low-cost alternative base isolation system by means of introducing infrastructure elements in the ground soil including wave barriers (Murillo et al., 2009), geosynthetic liners (Yegian & Catan, 2004), or rubber-soil mixtures (Senetakis et al., 2012). Although various investigations have focused on evaluating the dynamic performance of RSm (Zheng-Yi & Sutter, 2000; Mashiri et al. 2016), only a few studies have proposed shear modulus ( $G$ ) and damping ( $\xi$ ) - shear strain curves to predict the variation in the dynamic properties with the rubber content. This paper seeks to understand the fundamental dynamic behaviour of RSm by evaluating the variation in  $G$  and  $\xi$  from small-to-large strains.

## 2 EXPERIMENTAL PROGRAMME

### 2.1 Materials

The RSM used in this study comprises a coarse rounded to sub-rounded Leighton Buzzard sand (LBS), with  $d_{s50}=0.85$  mm; coefficient of uniformity,  $C_u=1.27$ ; and specific gravity,  $G_s=2.68$ . The rubber is obtained from car tyre sidewalls. Once all steel belts are removed, the rubber is devulcanised and then mechanically shredded. Rubber particle size  $d_{R50}=1.3$ mm, which is classified as rubber fibres according to ASTM 6270-12. Particle size distributions of both LBS and rubber particles are shown in Figure 1a. The rubber fibres exhibit the shape of small shreds particles (Figure 1b), with a typical length = 4mm and width = 2mm. These are going to be denoted shredded rubber (ShR) henceforth. Rubber  $G_s$  is taken to be 1.12 (Edil & Bosscher, 1994). Hence, the shredded rubber soil mixtures (ShRm) used in this study exhibit a relative size ratio around 1.5.

### 2.2 Equipment

A resonant column/torsional (RC) shear testing GCTS TSH-200 (at Indian Institute of Science, Bangalore) was employed to determine the dynamic properties of RSm at small strains. The equipment can vibrate the top of the soil specimen to frequencies up to 250 Hz by means of a torsional device connected to a torque transducer. The standard motor of the systems has a 2.3 Nm torque capacity and weighs 1.8 kg and the cell was pressurized by using a pneumatic pressure fluid. A cyclic triaxial (CT) testing rig was used to evaluate dynamic properties at medium-to-large strains. The operational frequency range of the CT equipment is between 0.01Hz and 10Hz. The apparatus consists of a 50kN capacity loading frame with a pneumatic actuator that provides a double amplitude axial displacement of 25mm (+/- 12.5mm). A linear variable differential transformer (LVDT) transducer is integrated in the actuator which is able to monitor precisely displacements of 0.001mm. Three standard pressure transducers are

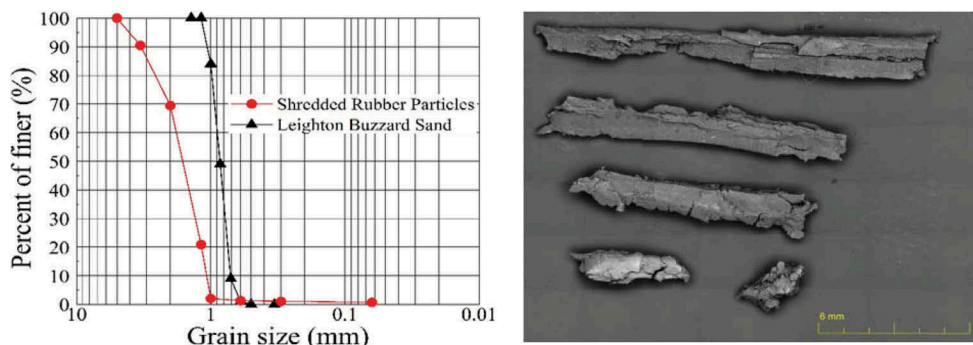


Figure 1. a) Sieve analysis of LBS and ShR and b) Microscopic image of ShR

contained in the equipment to measure the variation in cell pressure (CP), pore water pressure (PWP) and back pressure (BP).

### 2.3 Methods

Specimens tested in both RC and CT apparatus were 50 mm diameter and 100mm height at rubber percentages:  $\chi = 0, 10, 20$  and 30% by mass. Each specimen was prepared in four layers. To construct LBS samples, dry pluviation method was employed pouring dry particles through a cone funnel into the specimen mould. Alternatively, hand spooning method was used to form ShRm specimens due to the large dimensions of rubber particles. To avoid segregation of the smaller sand particles and thus ensure the homogeneity of the specimen, a 2.5% moisture content was introduced to each specimen. Afterward, sand particles and different rubber inclusions, depending on the rubber percentage, were mixed together and spooned into the cylindrical mould.

For testing cyclic triaxial tests, a water flow was introduced from the PWP valve, circulated through the sample and finally extracted using the BP valve. When Skempton pore-pressure parameter  $B (= \Delta U / \Delta \sigma)$  reached a value over 95%, the samples were considered to be saturated. After the saturation was completed, the samples were consolidated isotropically.

### 2.4 Test programme

The experimental programme consisted of a series of experiments carried out on ShRm (i.e.,  $\chi = 0-30\%$ ) in the RC, under dry conditions, and in the CT, under saturated undrained conditions. All samples were consolidated isotropically under a unique confining pressure (i.e.,  $\sigma_3 = 100$  kPa). The dynamic properties, shear modulus ( $G$ ) and damping ratio ( $\xi$ ), have been evaluated to understand the cyclic behaviour of both LBS and ShRm. In the RC, the dynamic behaviour of each rubber percentage was evaluated from the peak deformation of the specimen, at various torque forces, covering the small-to-medium shear strain range (i.e., 0.0001 - 0.2 %), following ASTM 4015-15. In the CT, saturated samples were subjected to strain controlled cycles (1 Hz) at specific shear strains in the medium-to-large range ( $\gamma = 0.05, 0.1, 0.2$ , and 1%).  $G$  and  $\xi$  have been determined by considering a specific hysteresis loop, out of all the cyclic loads applied to the material (ASTM 3999-11). For rigour purposes, the second cyclic loop (N) has been chosen to evaluate the dynamic properties of ShRm with CT.

## 3 RESULTS AND DISCUSSION

### 3.1 Shear modulus and damping ratio of ShRm

The variation in the shear modulus and damping ratio of ShRm with the rubber content at small-to-large strains ( $\gamma = 0.0001 - 1\%$ ) are shown in Figure 2. A reduction in soil shear stiffness  $G$ , both with shear strain and rubber content, can be seen. In common with previous works, this behaviour is explainable by the presence of highly deformable rubber particles (Zheng-Yi & Sutter, 2000; Senetakis et al., 2012; Bernal-Sanchez et al., 2018). The shear modulus at very small strains corresponds to the maximum shear stiffness  $G_0$  of an undisturbed soil. From Figure 2a, it is shown that  $G_0 = 111.8$  MPa, 52.3 MPa, 20.2 MPa, and 7.9 MPa for  $\chi = 0, 10, 20$  and 30%, respectively. Then  $G$  decays gradually for all rubber percentages when applying larger strain amplitudes (i.e.,  $\gamma > 0.2\%$ ) due to the soil disturbance. This phenomenon is observed to be more pronounced at  $\chi = 0, 10\%$ , as one would expect for a pure sand and RSm in which the sand fraction is dominant (Lee et al., 2010). On the other hand, the initial  $G$  and subsequent decrease with strain amplitude is lower in specimens containing a higher rubber content ( $\chi = 20 - 30\%$ ). This can be explained by the higher rubber content that confers on the mixture a marked compressibility, commonly known as the rubber-like behaviour of the mixture (Kim & Santamarina, 2008), and thus a greater ability to withstand the action of large deformations.

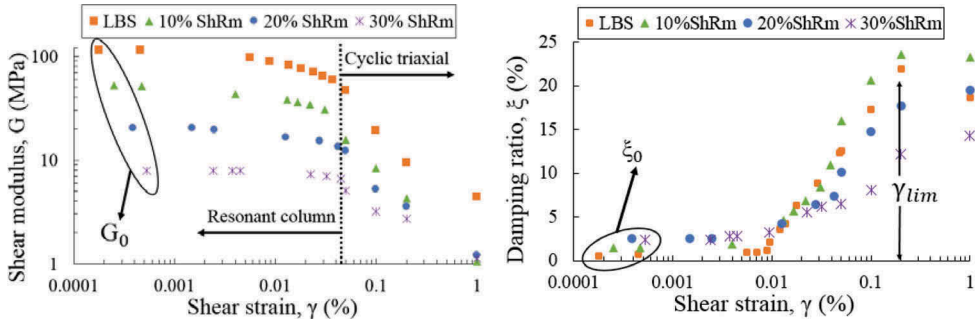


Figure 2. Variation in a) shear modulus and b) damping ratio with shear strain and rubber content at  $N = 2$

The change in  $\xi$  with the shear strain amplitude is shown in Figure 2b. The damping ratio increases in all tests with the application of greater strain amplitudes. At very small strains (i.e.  $\gamma = 0.0001$  %), there is an improvement in the minimum damping ratio  $\xi_0$  when adding more rubber. The value of  $\xi_0 = 0.52, 1.52, 2.51, 2.44\%$  corresponds to  $\chi = 0, 10, 20$ , and  $30\%$ . As established by previous investigations (Zheng-Yi & Sutter, 2000; Senetakis et al. 2012), the energy dissipation in RSm occurs due to the development of the friction through the particle sliding of sand particles in addition to the combination of friction and predominant deformation experienced by rubber particles. Therefore, in line with results obtained by Anastasiadis et al. (2012), there appears to be an upper limit in  $\xi_0$  attributed to (i) the size ratio between sand and rubber particles and (ii) amount of rubber introduced in the mixture. In the range  $\gamma = 0.01 - 0.1$  %, it is observed that the evolution of  $\xi$  exhibits a more linear increase with the amount of rubber. That said, it is difficult to distinguish between the pure sand and 10% ShRm. Beyond  $\gamma = 0.1$  or  $0.2\%$  the linear relationship breaks down, indeed the pure sand and 10%ShR point to an upper limit, even a reduction in damping, at high shear strains. This is attributable to the existence of a limiting shear strain  $\gamma_{lim}$ , defined as the strain at which the higher damping ratio is observed for mixtures, which appears to increase with the addition of rubber (Pistolas et al., 2018). Therefore, despite the reduction in  $\xi$  at  $\chi > 10\%$  (Anbazhagan & Manohar, 2015), the upper limit in  $\xi$  found in sand-like specimens contrasts with the increasing trend observed in the damping ratio of 20-30% ShRm. As established by Pistolas et al. (2018), this is due to the dislocation of rubber/sand particles, which leads to an interlocking mechanism due to the high interparticle-particle friction exhibited by rubber particles (e.g. Lopera Perez et al., 2016), reason why this phenomenon is more evident in rubber-like soils.

### 3.2 Normalise d shear modulus and damping ratio – shear strain curves for ShRm

A normalised shear modulus ( $G/G_0$ ) - shear strain curve was presented by Darendeli (2001). Equation 1 introduces the function parameter denoted as the curvature coefficient ( $a$ ), shown in Table 1, which depends on the number of cycles ( $N$ ) and the loading frequency:

$$G/G_0 = 1/(1 + (\gamma/\gamma_r)^a) \quad (1)$$

Where, reference strain  $\gamma_r$  is obtained from  $\gamma$  at  $G/G_0 = 0.5$ ,  $\gamma$  is the current shear strain value, and  $a$  is the curvature coefficient.

As shown in Table 1, the curvature coefficient and reference strain ( $\gamma_r$ ) have been estimated by applying the modified hyperbolic model on the experimental data. The reference strain maintains the same value with adding 10% ShR, but then it increases as rubber content increases. This indicates that the response of the mixture presents a more linear shape at  $\chi > 10\%$ . On the other hand, no clear trend of the rubber content on the curvature coefficient is observed, ranging between 1.31 and 1.42 for ShRm. Figure 3 depicts the adjusted curves for

Table 1. Curve fitting parameters for  $G/G_0$  – shear strain curves based on Darendeli (2001)

| Samples  | Reference strain, $\gamma_r$ (%) | a    | $R^2$ |
|----------|----------------------------------|------|-------|
| LBS      | 0.035                            | 1.17 | 0.966 |
| 10% ShRm | 0.034                            | 1.37 | 0.982 |
| 20% ShRm | 0.067                            | 1.42 | 0.994 |
| 30% ShRm | 0.106                            | 1.31 | 0.951 |

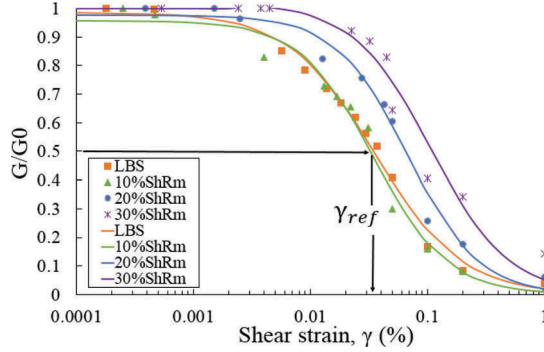


Figure 3. Normalised shear modulus versus shear strain of ShRm

each rubber percentage and the experimental results. Adding more than 10% ShR confers the mixture a more resilient state leading to a lower stiffness degradation, which is more evident at medium to large strains. Although Darendeli (2001) postulated this expression based on 200 dynamic tests performed on granular soils, the results shown in Figure 3 reveal a high correlation between the experimental data and the proposed expression (see Table 1), where  $R^2$  is in excess of 0.95 for all ShRm.

The variation in  $\xi$  with the shear strain amplitude has also been studied based on the non-linear hyperbolic model established by Darendeli (2001). This model is a modification of the original material damping – shear strain curve expressed by Masing (1926), which follows the commonly known Masing rules. Darendeli (2001) proposed the inclusion of  $\xi_0$  to overcome the underestimation observed in  $\xi$  at small strains when compared to the damping ratio obtained in experimental results. Furthermore, a reduction factor ( $DF(\gamma)$ ) was applied to the original Masing equation to adjust the evolution in the damping degradation based on the stiffness reduction  $G/G_0$  at medium-to-large strains. Equations 2-4 show the modified expression for determining the damping curve, which depends on the number of cycles and the normalised shear modulus:

$$\xi_{Darendeli} = DF(\gamma)\xi_{Masing} + \xi_0 \quad (2)$$

$$DF(\gamma) = b_1(G_\gamma/G_0)^{0.1} \quad (3)$$

$$b_1 = 0.6329 - 0.00057 \ln N \quad (4)$$

Where  $\xi_0$  = minimum damping ratio,  $G_0$  = maximum shear modulus,  $G_\gamma$  = current shear modulus.

It can be observed in Figure 4a that Darendeli's model provides a good fit at small-to-medium strains (i.e.,  $\gamma = 0.0001$ -0.05%). However, a different behaviour is observed between sand-like and rubber-like specimens at larger strains ( $\gamma > 0.05\%$ ). In other words, the expression appears to overestimate the damping ratio for 20-30% ShRm, whereas the opposite trend

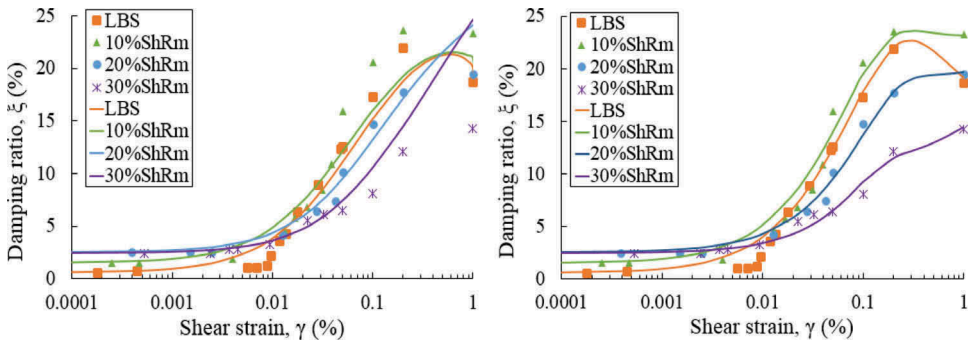


Figure 4. Damping ratio versus shear strain based on a) Darendeli (2001), b) Phillips & Hashash (2009)

Table 2. Curve fitting parameters based on Phillips & Hashash (2009)

| References | $p_1$ | $p_2$ | $p_3$ | $\xi_0$ (%) |
|------------|-------|-------|-------|-------------|
| LBS        | 0.65  | 0.32  | 15.71 | 0.52        |
| 10% ShRm   | 0.67  | 0.28  | 17    | 1.52        |
| 20% ShRm   | 0.6   | 0.38  | 11    | 2.51        |
| 30% ShRm   | 0.5   | 0.7   | 6.5   | 2.44        |

occurs with LBS and 10% ShRm. The function postulated by Darendeli (2001) was created on the basis of the dynamic tests performed on partially saturated granular soils. This might explain why this expression does not provide a good fit at larger strains, where the behaviour of ShRm is more unpredictable. A different approach may be obtained using the equation postulated by Phillips & Hashash (2009). An alternative reduction factor is used which depends on the normalised shear modulus and three curve fitting parameters. This model is known as the Pressure-Dependent Hyperbolic model which provides a better fit of the damping curve by matching the empirical results with the original expression proposed by Masing (1926). Equations 5-6 describe the modified expression:

$$\xi_{Hashash} = F(\gamma)\xi_{Masing} + \xi_0 \quad (5)$$

$$F(\gamma) = p_1 - p_2(1 - (G_\gamma/G_0))^{p_3} \quad (6)$$

Where,  $p_1$ ,  $p_2$ , and  $p_3$  are curve fitting parameters.

Table 2 shows the parameters estimated for each LBS and ShRm to depict the damping curves traced in Figure 4b. It can be observed that the curve fitting parameters ( $p_1$ ,  $p_2$ ,  $p_3$ ) are nearly similar for LBS and 10% ShRm. At  $\chi > 10\%$ , the evolution in the values of  $p_1$  and  $p_3$  follow a decreasing trend, whereas  $p_2$  increases. Hence, Equations 7-9 have been proposed in this study to determine the value of  $p_1$ ,  $p_2$ ,  $p_3$  and thus apply to Equation 6 depending on the rubber content:

$$p_1 = -0.0003 (\chi^2) + 0.0038 (\chi) + 0.653 \quad (7)$$

$$p_2 = 0.0009 (\chi^2) - 0.0146 (\chi) + 0.324 \quad (8)$$

$$p_3 = -0.0145 (\chi^2) + 0.0979 (\chi) + 16.15 \quad (9)$$

Where,  $\chi$  is the rubber percentage by mass.

The reduction factor ( $F(\gamma)$ ) adjusts the damping curve to the empirical values providing a better fit than the damping curves adapted from Darendeli's hyperbolic model (i.e., Figure 3a). It can therefore be observed that the new expression identifies the decay in the value  $\xi$  for LBS and 10% ShRm, as well as a gradual increase in  $\xi$  is predicted at  $\chi = 20\text{-}30\%$  for very large strains.

## 4 CONCLUSIONS

In the present study, the dynamic behaviour of shredded rubber soil mixtures (ShRm), considering different rubber inclusions ( $\chi = 0\text{-}30\%$ ), has been evaluated from small to large deformations ( $\gamma = 0.0001 - 1\%$ ) by means of resonant column and cyclic triaxial tests.

It has been observed that the shear modulus of ShRm decreases with the shear strain and the rubber content. On the other hand, the elasticity of shredded rubber (ShR) confers the mixture a greater ability to withstand large deformations leading to a lower stiffness degradation. The normalised shear modulus – shear strain functional model established by Darendeli (2001) provides a good fit with the experimental results of ShRm at any rubber percentage.

The minimum damping ratio  $\xi_0$  increases with the amount of ShR attributed to the development of the friction between sand particles and the predominant deformation experienced by rubber particles, as established by Senetakis et al. (2012). Then,  $\xi$  increases at a higher rate in sand-like soils (i.e., LBS and 10% ShRm), whereas a more linear evolution is exhibited by rubber-like soils (i.e., 20 and 30% ShRm). Although the damping ratio – shear strain curve expression postulated by Darendeli (2001) provides a good fit at small-to-medium strains, this does not appear to predict accurately the variable behaviour of ShRm at large strains. Instead, the model proposed by Phillips and Hashash (2009) has been introduced, adapting the curve fitting parameters to the empirical values of ShRm, providing a better fit than Darendeli's expression.

## ACKNOWLEDGEMENTS

The work reported on in this paper was made possible through the award Newton Bhabha PhD Placement Programme granted by the British Council and the Department of Science and Technology. It enabled the lead author to spend 2 months working with Prof P. Anbazhagan and colleagues utilizing advanced testing equipment at the Indian Institute of Science, Bangalore. All authors are grateful for the support provided during this period.

## REFERENCES

- Anastasiadis, A., Senetakis, K. & Ptilakis, K. 2012. Small-strain shear modulus and damping ratio of Sand-rubber and gravel-rubber mixtures. *Geotechnical and Geological Engineering* 30(2), pp. 363–382. DOI: 10.1007/s10706-011-9473-2.
- Anbazhagan, P. & Manohar, D.R. 2015. Energy absorption capacity and shear strength characteristics of waste tire crumbs and sand mixtures. *International Journal of Earthquake Geotechnical Engineering* 6(1).
- Anbazhagan, P., Manohar, D.R. & Rohit, D. 2017. Influence of size of granulated rubber and tyre chips on the shear strength characteristics of sand-rubber mix. *Geomechanics and Geoengineering* 12(4), pp. 266–278. DOI: 10.1080/17486025.2016.1222454.
- ASTM D3999. 2011. Standard Test Methods for the Determination of the Modulus and Damping Properties of Soils Using the Cyclic Triaxial Apparatus. ASTM International, West Conshohocken.
- ASTM D4015. 2015. Standard test methods for modulus and damping of soils by fixed-base resonant column devices. ASTM International, West Conshohocken.
- ASTM D6270. 2012. Standard practice for use of scrap tires in civil engineering applications.
- Bernal-Sanchez, J., McDougall, J., Barreto, D., Miranda, M., Marinelli, A. 2018. Dynamic behaviour of shredded rubber soil mixtures. *16<sup>th</sup> European Conference on Earthquake Engineering, Thessaloniki*.



- Darendeli, M.B. 2001. Development of a new family of normalized modulus. *CEUR Workshop Proceedings* 1542(9), pp. 33–36. DOI: 10.1017/CBO9781107415324.004.
- Edil, T.B. & Bosscher, P.J. 1994. Engineering properties of tire chips and soil mixtures. *Geotechnical Testing Journal* 17(4): 453.
- Ehsani, M., Shariatmadari, N. & Mirhosseini, S.M. 2015. Shear modulus and damping ratio of sand-granulated rubber mixtures. *J. Cent. South Univ* 22, pp. 3159–3167. DOI: 10.1007/s11771-015-2853-7.
- ETRMA. 2015. *End-of-life tyre report 2015*.
- European Union. 2006. Implementation of the landfill directive at regional and local level. Luxembourg, Office for Official Publications of the European Communities.
- Ghazavi, M. 2004. Shear strength characteristics of sand-mixed with granular rubber. *Geotechnical and Geological Engineering* 22(3), pp. 401–416. DOI: 10.1023/B:GEGE.0000025035.74092.6c.
- Hazarika, H., Kohama, E. & Sugano, T. 2008. Underwater shake table tests on waterfront structures protected with tire chips cushion. *Journal of Geotechnical and Geoenvironmental Engineering* 134(12), pp. 1706–1719. DOI: 10.1061/(ASCE)1090-0241(2008)134:12(1706).
- Kaneko, T., Orense, R.P., Hyodo, M. & Yoshimoto, N. 2013. Seismic response characteristics of saturated sand deposits mixed with tire chips. *J. Geotech. Geoenviron. Eng.* 139(4), pp. 633–643.
- Kim, H.K. & Santamarina J.C. 2008. Sand-rubber mixtures (large rubber chips). *Canadian Geotechnical Journal*. 45, pp. 1457–1466.
- Lee, C., Truong, Q., Lee, W. & Lee, J.S. 2010. Characteristics of rubber-sand particle mixtures according to size ratio. *Journal of Materials in Civil Engineering* 22, pp. 323–331.
- Lopera Perez, J.C., Kwok, C.Y. & Senetakis, K. 2016. Effect of rubber size on the behaviour of sand rubber mixtures: A numerical investigation. *Computers and Geotechnics*. DOI: 10.1016/j.compgeo.2016.07.005
- Mashiri, M.S., Vinod, J.S. & Sheikh, M.N. 2016. Liquefaction potential and dynamic properties of sand-tyre chip (STCh) mixtures. *Geotechnical Testing Journal*. DOI: 10.1520/GTJ20150031.
- Masing, G. 1926. *Spannung und Verfestigung Beim Masing*. *Proceedings, Second International Congress of Applied Mechanics* 7, pp. 332–335.
- Murillo, C., Thorel, L. & Caicedo, B. 2009. Ground vibration isolation with geofam barriers: Centrifuge modeling. *Geotextiles and Geomembranes* 27(6), pp. 423–434. DOI: 10.1016/j.geotextmem.2009.03.006.
- Phillips, C. & Hashash, Y.M.A. 2009. Damping formulation for nonlinear 1D site response analyses. *Soil Dynamics and Earthquake Engineering* 29(7), pp. 1143–1158. DOI: 10.1016/j.soildyn.2009.01.004.
- Pistolas, G.A., Anastasiadis, A. & Pitilakis, K. 2018. Dynamic behaviour of granular soil materials mixed with granulated rubber: Effect of rubber content and granularity on the small-strain shear modulus and damping ratio. *Geotechnical and Geological Engineering* 36(2), pp. 1267–1281.
- Senetakis, K., Anastasiadis, A., & Pitilakis, K. 2012. Dynamic properties of dry sand/rubber (SRM) and gravel/rubber (GRM) mixtures in a wide range of shearing strain amplitudes. *Soil Dynamics and Earthquake Engineering* 33(1), pp. 38–53. DOI: 10.1016/j.soildyn.2011.10.003.
- Sheikh, M.N., Mashiri, M.S., Vinod, J.S., & Tsang, H.H. 2012. Shear and Compressibility Behaviour of Sand-Tyre Crumb Mixtures. *Journal of Materials in Civil Engineering* 25(10), pp. 1366–1374.
- Spence, R.J.S., So, E. & Scawthorn, C. 2011. Human casualties in earthquakes: progress in modelling and mitigation.
- Tsang, H.H. 2008. Seismic isolation by rubber-soil mixtures for developing countries. *Earthquake Engineering and Structural Dynamics* 37(2), pp. 283–303. DOI: 10.1002/eqe.756.
- Yegian, M. & Catan, M. 2004. Soil isolation for seismic protection using a smooth synthetic liner. *Journal of Geotechnical and Geoenvironmental Engineering* 130(11), pp. 1131–1139.
- Youwai, S. & Bergado, D.T. 2003. Strength and deformation characteristics of shredded rubber tire sand mixtures. *Canadian Geotechnical Journal* 40(2), pp. 254–264. DOI: 10.1139/t02-104.
- Zheng-Yi, F. & Sutter, K.G. 2000. Dynamic properties of granulated rubber/sand mixtures. *Geotechnical Testing Journal* 23(3), pp. 338–344.